

Provided for non-commercial research and education use.
Not for reproduction, distribution or commercial use.



This article appeared in a journal published by Elsevier. The attached copy is furnished to the author for internal non-commercial research and education use, including for instruction at the authors institution and sharing with colleagues.

Other uses, including reproduction and distribution, or selling or licensing copies, or posting to personal, institutional or third party websites are prohibited.

In most cases authors are permitted to post their version of the article (e.g. in Word or Tex form) to their personal website or institutional repository. Authors requiring further information regarding Elsevier's archiving and manuscript policies are encouraged to visit:

<http://www.elsevier.com/copyright>



Contents lists available at SciVerse ScienceDirect

International Journal of Heat and Mass Transfer

journal homepage: www.elsevier.com/locate/ijhmt

The effects of surfactant monolayers on free surface natural convection

S.M. Bower*, J.R. Saylor

Clemson University, Department of Mechanical Engineering, Clemson, SC 29634-0921, United States

ARTICLE INFO

Article history:

Received 1 June 2011

Received in revised form 26 July 2011

Accepted 26 July 2011

Available online 29 August 2011

Keywords:

Natural convection

Free surface

Nusselt

Rayleigh

Surfactant

ABSTRACT

An experimental investigation of the effects of surfactant monolayers on free surface natural convection is presented in which the Rayleigh number, Ra , is used to parameterize the Nusselt number, Nu , with the power law scaling $Nu = A \cdot Pr^m Ra^n$. Experiments were conducted in water under the following free surface conditions: (1) clean surface, (2) oleyl alcohol covered surface, (3) stearic acid covered surface, and (4) stearyl alcohol covered surface. The use of an infrared (IR) camera permitted confirmation of these surface conditions and the measurement of the surface temperature. The results reveal a reduction of Nu by approximately one order of magnitude in the presence of any of the three surfactants investigated, compared to the clean surface at equivalent Ra . This reduction in convective ability is attributed to the shear-yielding hydrodynamic boundary condition imposed by the monolayers compared to the shear free condition of the clean surface. All four surface conditions yield an exponent $m > 1/3$, which is attributed to a relatively non-homogeneous temperature boundary condition at the free surface compared to the boundary condition of a Rayleigh–Bénard study. A dependence of Nu upon aspect ratio Γ was also discovered in contrast to earlier work which suggested that Nu is independent of Γ , at least for large Γ .

© 2011 Elsevier Ltd. All rights reserved.

1. Introduction

This investigation is focused on how surfactant monolayers affect natural convection in a body of water confined from above by a free surface. The physical situation which motivates this heat transfer problem is that of a heated body of water for which the bulk water temperature T_b is greater than that of the air T_∞ . Evaporation acts primarily to cool the surface temperature T_s below the temperature of the underlying bulk water. The water-side temperature difference ΔT causes a buoyancy-driven flow which results in natural convection heat transfer in the water. While natural convection also occurs in the air above a heated body of water, this is not the subject of the present study.

The free surface considered here is an air/water interface, across which both heat and mass transfer (i.e. evaporation) can occur. In the absence of surfactants, this free surface has a shear-free hydrodynamic boundary condition [1,2] in contrast to the no-slip boundary condition of a solid wall in the classical Rayleigh–Bénard convection problem. Strictly speaking, a free surface can experience finite shear from the movement of air above the interface; this effect is not considered here due to the very small air velocities present above the water surface. The convective behavior of a heated water body bound by a free upper surface is important to environmental flows which occur in inland bodies of water such as lakes, ponds, reservoirs, and industrial cooling impoundments.

It is therefore surprising that a great majority of natural convection studies are focused on the traditional Rayleigh–Bénard rigid–rigid boundary problem. As an aside, the authors note that in addition to Rayleigh–Bénard and free surface natural convection discussed here, there are many other convective scenarios for different geometries. As just one example, Lau et al. [3] examined natural convection in a vertical parallel-plate channel where one of the plates was heated. A review of the natural convection literature can be found in Goldstein et al. [4].

Free surface natural convection in water can be complicated by the presence of a surfactant monolayer. These monomolecular films affect the air/water interface in several ways; they lower surface tension σ and in some instances inhibit evaporation [5]. Of special interest to the work presented here is the fact that surfactant monolayers introduce compressibility to the air/water interface, which would otherwise be absent, thereby permitting shear at the interface. The compressibility, C , is defined as:

$$C = -\frac{1}{a} \left(\frac{\partial a}{\partial \pi} \right)_T \quad (1)$$

where a is the molecular area of the film, and π is the surface pressure defined as:

$$\pi = \sigma_0 - \sigma \quad (2)$$

where σ_0 and σ are the surface tensions of a clean free surface and a monolayer covered surface, respectively ($\sigma_0 = 72.0$ mN/m at $T = 25^\circ\text{C}$ [6]). The compressibility C characterizes a monolayer's tendency to resist compression, and is related to the Gibbs elasticity

* Corresponding author. Tel.: +1 913 961 2148; fax: +1 864 656 4435.

E-mail address: bower@clemson.edu (S.M. Bower).

Nomenclature

A	Nu – Ra power law coefficient	β	coefficient of volumetric expansion (K^{-1})
C	compressibility (m/mN)	Γ	aspect ratio, W/D
c_p	specific heat (J/kgK)	ν	kinematic viscosity (m^2/s)
D	tank depth (m)	π	surface pressure (mN/m)
g	gravitational acceleration (m/s^2)	ρ	density (kg/m^3)
h	heat transfer coefficient (W/m^2K)	σ	surface tension (mN/m)
\mathcal{H}	heat transfer coefficient ratio		
k	thermal conductivity ($W/m K$)		
m	Nu – Ra power law exponent	Subscripts	
\dot{m}''	evaporative mass flux (kg/m^2s)	b	bulk water
Ma	Marangoni number	c	convection
n	Prandtl number exponent	∞	ambient
Nu	Nusselt number	o	clean free surface
Pr	Prandtl number	s	surface
q''	heat flux (W/m^2)	t	total
Ra	Rayleigh number	w	wall
Sh	Sherwood number		
T	temperature ($^{\circ}C$)	Superscripts	
W	tank width (m)	\dagger	free surface equivalent
		$*$	evaluated at \bar{m}
Greek Symbols			
α	thermal diffusivity of liquid water (m^2/s)		

E through the reciprocal [7]. If a water surface is completely devoid of surfactants, $C \rightarrow \infty$ since there is no variation in π with molecular area [7], and the surface is free of shear. Hereforward, we will refer to a surface that is free of surfactant material as a clean surface.

Naturally occurring organic surface films are ubiquitous on inland bodies of water [8]; it is therefore important to study their role in the convective process, which to date is not well understood. In the present work, we study natural convection in both the presence and absence of surfactant material hypothesizing that a surfactant effects an intermediary boundary condition between the extremes of a clean free surface and a solid wall.

Jarvis [9,10] studied the effects of cetyl alcohol and oleic acid monolayers on the temperature below a free surface. Thermistors were placed at depths of 2, 30, and 150 mm below the surface of a water tank which was maintained at approximately $20^{\circ}C$. Dry nitrogen and air at 55% relative humidity were separately passed over the surface at flow rates from 1 to 6 liters/minute in order to observe a range of evaporative behavior. The interface was swept several times with a movable barrier to achieve a clean surface. When a monolayer of cetyl alcohol was added to the clean surface with a low flow rate of dry nitrogen, the surface temperature probe at 2 mm depth measured an increase in temperature T_s of approximately $0.5^{\circ}C$ relative to the clean surface case. Jarvis attributed this surface warming effect to the ability of cetyl alcohol to retard evaporation (this behavior was not seen with oleic acid). Additionally, the magnitude of temperature fluctuations 2 mm below the free surface was significantly reduced when the cetyl alcohol was added to the clean air/water interface. Jarvis explains qualitatively that the large fluctuations under the clean surface are indicative of the rapid convective exchange, and that the cetyl alcohol inhibits the water motion in the immediate surface region. In a second experiment, air was passed over a clean free surface at an increased rate of 6 liters/minute, which caused T_b and T_s to be approximately equal due to the mixing of the bulk fluid induced by the surface shear. When either oleic acid or cetyl alcohol was added to the free surface, T_s became depressed below T_b by approximately $0.4^{\circ}C$. Jarvis concluded that the presence of the monolayers retards the convective motion and immobilizes a thin layer of water at the surface allowing it to cool. Throughout the experiments of Jarvis, T_b was essentially the same for the clean surface

and surfactant-covered conditions. This behavior indicates that the convection-inhibiting effect of the monolayers is limited to a thin layer below the surface. A later study by Katsaros and Garrett [11] showed similar results.

Flack et al. [2] investigated the turbulence of the near surface region in a heated water body ($T_b \approx 40^{\circ}C$) using laser Doppler velocimetry (LDV). Experiments were conducted by measuring two components of velocity at various depths beneath a clean surface and an oleyl alcohol covered surface. Flack et al. regarded the clean surface as being shear free, and considered that a monolayer of oleyl alcohol imparts a constant elasticity boundary condition at the surface. Time traces of the horizontal velocity (i.e. in the surface plane) at a depth of 0.5 mm were obtained which show that the large amplitude fluctuations observed under the clean free surface are reduced significantly with the introduction of the oleyl alcohol surfactant at equivalent heat fluxes. The difference in the vertical velocities beneath the two surface conditions was less dramatic, owed to the zero vertical velocity requirement at the air/water interface. When the same measurements were made at an increased depth of 4 mm, the difference between the clean free surface and oleyl alcohol surface was less distinct. Flack et al. conclude that the ability of oleyl alcohol to dampen subsurface motion is limited to the first 4 mm of the surface sublayer region. These results support what Jarvis [10] had observed with surface temperature fluctuations beneath a clean free surface and a cetyl alcohol covered surface.

The Nusselt and Rayleigh numbers are used to characterize the convective heat transfer q_c'' and the state of turbulence in natural convection, respectively. The Nusselt number Nu is defined as:

$$Nu = \frac{hD}{k} \quad (3)$$

where D is the vertical extent of the fluid layer, k is the thermal conductivity of the fluid, and h is the heat transfer coefficient defined as:

$$h = \frac{q_c''}{\Delta T} \quad (4)$$

Here q_c'' is the convective heat flux and ΔT is the characteristic temperature difference across the fluid layer.

In the traditional Rayleigh–Bénard setup, ΔT is the temperature difference between two isothermal hot and cold plates. In the present work, ΔT is defined with respect to the unsteady, non-penetrative convection problem of a fluid that is cooling at the free surface:

$$\Delta T = T_b - \bar{T}_s \quad (5)$$

where T_b is the bulk water temperature and \bar{T}_s is the spatially averaged surface temperature. It is assumed here that the temperature of the insulated bottom surface is equivalent to T_b . A schematic of the physical differences between the Rayleigh–Bénard setup and the problem studied here is presented in Fig. 1. The Rayleigh number, Ra , is used as a measure of the strength of the convective flow:

$$Ra = \frac{g\beta\Delta T D^3}{\nu\alpha} \quad (6)$$

where g is the gravitational acceleration, β is the volumetric expansivity, and ν and α are the kinematic viscosity and thermal diffusivity of the fluid.

Natural convection heat transfer is often studied using the non-dimensional Nusselt–Rayleigh, or Nu – Ra , power law parameterization:

$$Nu = A \cdot Pr^n Ra^m \quad (7)$$

The Prandtl number is defined as $Pr = \nu/\alpha$. The coefficient A and the exponents n and m have long been a topic of study. Globe and Dropkin [12], for example, conducted experiments with water, mercury, and silicone oils to cover the range $0.02 < Pr < 8750$ and $1.51 \times 10^5 < Ra < 6.76 \times 10^8$ to determine A , n , and m in Eq. (7). For the present study with water, $3.9 < Pr < 5.1$ due to the temperature dependence of ν and α . This relatively narrow range of Pr makes the critical determination of n in Eq. (7) difficult and the interpretation becomes trivial. Often, when variation in Pr is small, Pr is simply absorbed into the coefficient A such that Eq. (7) appears as $Nu = A \cdot Ra^m$. Herein, the authors adopt the Pr exponent from the study of Globe and Dropkin [12] which, to the authors' knowledge, is the only Nu – Ra study to have investigated variation in Pr so extensively. The Nu – Ra parameterization used here is thus:

$$Nu = A \cdot Pr^{0.074} Ra^m \quad (8)$$

Navon and Fenn [13] studied evaporation and natural convection in the presence of surfactant monolayers using the Nu – Ra power law parameterization in Eq. (8). Experiments were performed in a shallow water trough (2 cm deep) by measuring the evaporative flux \dot{m}''

as the water bulk T_b warmed from 2 to 22 °C. Navon and Fenn chose to investigate this range of temperatures so that the density inversion of water could be observed at 4 °C. The air/water interface was swept clean with a Teflon barrier prior to experiments to achieve a clean free surface. The evaporative heat flux q_e'' was determined by measuring \dot{m}'' ; Navon and Fenn related this quantity to the convective heat flux q_c'' leaving the water, and Nu was subsequently computed. For temperatures greater than 4 °C, Navon and Fenn computed Nu and Ra which showed that $Nu \propto Ra^{1/3}$ (the coefficient A is not presented) for $Ra > 1.5 \times 10^4$. This result was comparable to the Nu – Ra findings of Federico and Foraboschi [14] who found $Nu = 0.092Ra^{1/3}$ for convection beneath an air/water interface for $Ra > 2.2 \times 10^4$. The surface condition in the study of Federico and Foraboschi was not explicitly controlled, however, and thus an uncontrolled/unknown surfactant monolayer was likely present instead of having a clean free surface. The Nu – Ra result due to Navon and Fenn was the first of its kind for a clean free surface.

In a companion paper, Navon and Fenn [15] investigated the role of cetyl alcohol and stearic acid surfactant monolayers on evaporation and natural convection within water. The same experimental facility was used as in the clean free surface Nu – Ra study [13]. Experiments were conducted in which each surfactant was applied to the free surface, and the monolayer was compressed with a barrier to increase the surface pressure π (Eq. (2)) incrementally while \dot{m}'' was measured. This process was conducted for temperatures T_b ranging from 2 to 22 °C. Navon and Fenn show that the evaporative resistance r of both monolayers increases with π which agrees with the findings of other studies [8,11,16–18]. Importantly, Navon and Fenn found that for $T_b > 4$ °C, Nu decreased with increasing surface pressure π when a cetyl alcohol monolayer was present at the interface. Navon and Fenn questioned whether the reduction in Nu was due simply to the increased retarding effect of π on \dot{m}'' , or if natural convection was directly inhibited by the presence of the monolayer. To answer this, Navon and Fenn used the Nu – Ra power law result from their earlier study of convection under a clean free surface [13] where it was found that $Nu \propto Ra^{1/3}$. Nu data from the cetyl alcohol condition were compared to Nu that would be expected at equivalent Ra for a clean surface according to their Nu – Ra relationship. The results show that Nu for the cetyl alcohol condition are less than Nu that would be expected for a clean surface. This clever manipulation of data suggests that the presence of a cetyl alcohol monolayer will directly inhibit the ability of the water to transfer heat via convection. In support of this idea, an increase in surface pressure π via film compression had seemingly no effect on Nu when $T_b = 2$ °C when convective motion was absent (i.e. for $T_b < 4$ °C the density inversion of water caused the fluid to become stably stratified). Thus, there was no convective motion for the monolayer to affect. Navon and Fenn conclude that Nu depends strongly on the boundary conditions at the surface, and that the cetyl alcohol monolayer behaves like a rigid boundary at the surface due to its low compressibility.

The argument Navon and Fenn present for cetyl alcohol is contradicted by their stearic acid data. At certain temperatures, Nu actually increases with surface pressure π indicating that the presence of the monolayer somehow enhanced convective exchange. Navon and Fenn posit that local convection cells near the thermocouples may have caused this apparent behavior, or that perhaps the effect was caused by the “squeezing out” of impurities in the stearic acid film as the monolayer was compressed. Because of the disagreement between the cetyl alcohol and stearic acid data, it is difficult to accept or reject the hypothesis of Navon and Fenn that the presence of a monolayer will directly inhibit natural convection by changing the hydrodynamic boundary condition at the surface. The shallow depth of the trough, 2 cm, and low range of Ra brings to question the relative importance of surface tension (i.e. Marangoni) effects on the convective flow. Furthermore, the

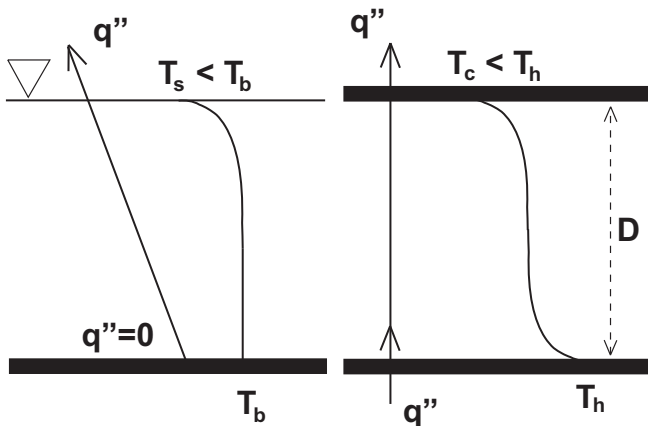


Fig. 1. Unsteady non-penetrative convection bounded by an insulated wall and free surface (the case studied here), and (right) steady, Rayleigh–Bénard convection between two isothermal plates with constant heat flux q_c'' , adapted from Adrian et al. [39].

range of Ra explored by Navon and Fenn is not characteristic of what would be expected in an environmental water body. Finally, Navon and Fenn did not consider the situation where $T_b > T_\infty$. More work is therefore needed to clarify the effect of surfactants on free surface natural convection.

Katsaros et al. [19] experimentally developed a Nu – Ra power law scaling for natural convection in a warm water tank with a free surface. A resistive thermal device was used to measure the temperature profile within the water, and an infrared radiometer was used to measure T_s . The interface was cleaned by skimming the indigenous surface film with a tissue, and measurements were subsequently acquired while the fluid cooled for at least one hour. The convective heat flux q_c' was computed from the time-rate-change of T_b , and the heat loss through the insulated tank walls was accounted for. Katsaros et al. found that $Nu = 0.156Ra^{0.33}$ under a clean surface for $4 \times 10^8 < Ra < 4 \times 10^9$. The effects of surfactant monolayers on natural convection were not investigated.

To the authors' knowledge, the only experimental clean surface studies which present the Nu – Ra parameterization are those of Navon and Fenn [13], and Katsaros et al. [19]. Although both of these studies claim to have a clean surface condition, there is reason to question whether this is truly the case. In both of these works the interface was swept with a Teflon barrier or tissue. Though never explicitly stated in the papers, we assume that the existence of the clean free surface was verified with either a Wilhelmy plate or DuNoüy ring and tensiometer device (a clean free surface will measure $\sigma = 70.5$ dynes/cm [20]). In the works of Navon and Fenn and Katsaros et al. no mention is made whether or not the surface condition was monitored during or after experimental runs to ensure that the free surface condition remained valid. The authors' own experience has shown that a clean surface is very difficult to preserve for more than about five minutes even when painstaking effort is made to maintain proper experimental procedure and cleaning methods [1,20,2,21]. Moreover, Saylor [20] has shown that significant surfactant contamination can occur without any measurable change in surface tension. Katsaros et al. have assumed the existence of a clean free surface for runs lasting at least one hour; they also state that some surfactant material was likely present though Katsaros et al. believe that the results were not affected [19].

This experimental difficulty of maintaining a clean, free surface makes important the need to verify the surface condition *in situ* during an experiment. The use of an infrared (IR) camera to visualize the air/water interface and ascertain the presence of surfactants has been done by Saylor [20] and Saylor, Smith, and Flack [2,21,22,1]. In the IR, there is a clear visual distinction between a clean free surface, and a surfactant covered surface. Herein, an IR camera is

employed to verify the existence of specific surface conditions, namely a clean free surface, with certainty. A sample pair of IR images of a clean surface and a surfactant-covered surface are presented in Fig. 2.

This study aims to make clear the physical effects of surfactant monolayers on natural convection within a heated water body. The investigations due to Jarvis [9,10] and Flack et al. [2] indicate that turbulent fluctuations in temperature and velocity in the subsurface region can be damped by the presence of a surfactant monolayer. Navon and Fenn [13] determined $Nu \propto Ra^{1/3}$ for a free surface at relatively low Ra , and conducted experiments [15] which suggest that surfactant monolayers directly inhibit convection by altering the hydrodynamic boundary condition at the surface. But because their cetyl alcohol and stearic acid results did not both agree with their hypothesis, their theory remains speculative. Katsaros et al. [19] later determined a Nu – Ra power law scaling for a clean free surface, but did not study the impact of surfactants on convection. It is unclear whether or not the results due to Navon and Fenn [13] and Katsaros et al. [19] are actually for a clean surface condition due to the described difficulty of conducting a surfactant-free experiment. The results from these studies reveal that surfactants can change the convective behavior of a fluid by affecting the hydrodynamic conditions at the surface, but more work is needed to explain the underlying physical mechanisms that are involved and to clarify the behavior of a true clean free surface.

To the authors' knowledge, this is the only comprehensive investigation of the effect of surfactant monolayers on Nu – Ra scaling for a liquid layer undergoing turbulent natural convection.

2. Experimental method

Experiments were conducted in a laboratory environment with insulated glass tanks filled with warm water. During an experiment, the water was allowed to cool down under a specific surface condition while T_b , \bar{T}_s , and T_∞ data were collected from which Nu and Ra were subsequently computed. The surface conditions were imposed by applying surfactant monolayers of (1) oleyl alcohol, (2) stearic acid, and (3) stearyl alcohol, and by removing all indigenous material to obtain (4) a clean surface. A schematic of the experimental facility is shown in Fig. 3.

The tanks were constructed of glass and sealed with silicone RTV. The outside walls were insulated with 4 cm foam to minimize heat loss. Seven tanks of varying depth D and width W were used, and these are summarized in Table 1 which also provides the aspect ratio Γ for each of the tanks, where Γ is defined as:

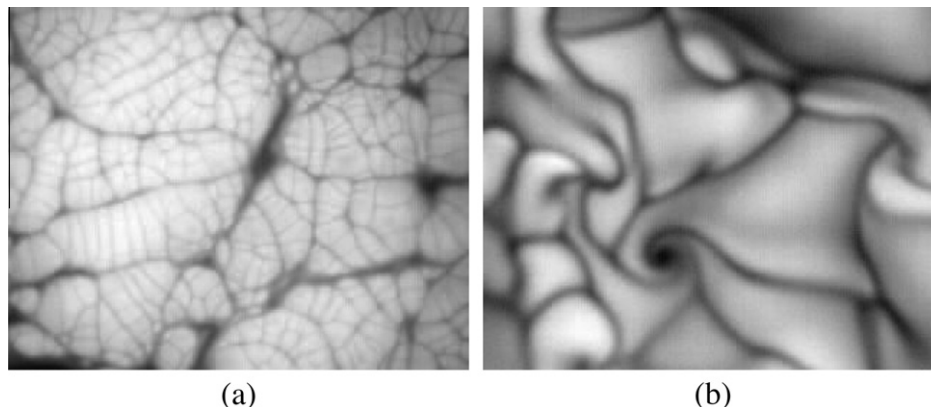


Fig. 2. IR images of a water surface: (a) in the absence of surfactant material, i.e. clean, and (b) in the presence of a surfactant monolayer (oleyl alcohol). For both images, the temperature of the underlying water is $T_b \approx 37$ °C, and the viewing area is approximately 7.6×5.7 cm.

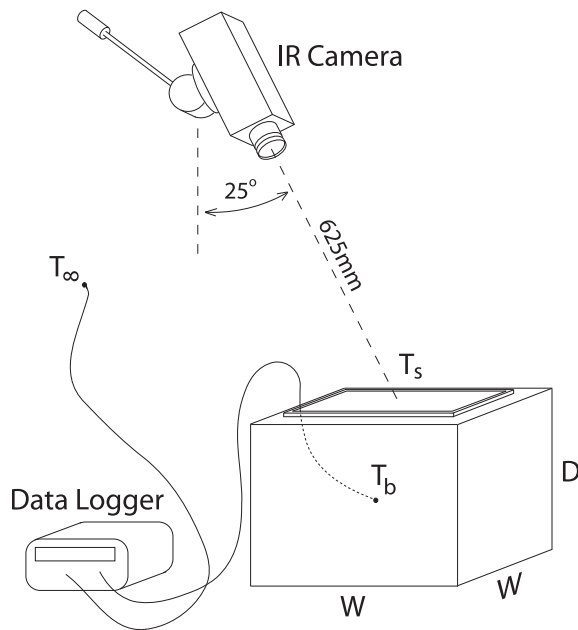


Fig. 3. The experimental facility with the insulated glass tank, the T_b and T_∞ data logger, the T_b probe inserted into the center of the water bulk, the T_∞ probe in the ambient, and the tripod-mounted IR camera for \bar{T}_s measurement.

Table 1
The aspect ratios $\Gamma = W/D$ for each of the tanks used in these experiments.

		Depth D			
		5 cm	10.1 cm	15.2 cm	35.5 cm
Width W	15.2 cm	3	–	–	–
	30.4 cm	6	3	2	0.86
	45.6 cm	9	–	–	–
	60.8 cm	12	–	–	–

$$\Gamma = W/D \quad (9)$$

The tanks were all square in footprint. The combination of depths D used herein allowed for a Rayleigh number range of $2 \times 10^6 < Ra < 3 \times 10^9$. The different tank widths served as part of the parameter space in an evaporation study that was conducted concurrently with this $Nu-Ra$ work, and is reported elsewhere.

The temperatures T_b and T_∞ were measured with a Fluke 5611T thermistor (± 0.01 °C) and a General Electric CSP60BA103M-H/2-90 thermistor (± 0.01 °C), respectively. The T_b and T_∞ data were logged at a rate of 1 Hz with a Hart Scientific 1529 Chub-E4 Thermometer Readout (± 0.002 °C accuracy and 0.0001 °C resolution). The T_b probe was inserted into the water at the edge of the tank and was positioned near the geometric center of the water bulk. The T_∞ probe was located far away from the vicinity of the cooling tank such that the measurement of T_∞ was not affected by the relatively warm plumes of air rising above the water surface.

An M-Wave IR camera (model MW320F4 from IR Cameras Infra-red Imaging Systems) was used to obtain images of the surface temperature field at a rate of 3 Hz. The camera was fixed to a tripod and located above the tank at an angle of 25° from vertical, and at a distance of 625 mm from the lens to the center region of the water surface. The observed surface region was approximately 7.6×5.7 cm with an image resolution of 42 pixels/cm. The camera detector was a 320×240 indium antimonide focal plane array (noise equivalent $\Delta T = 0.015$ K), which is sensitive to light in the 1.5–5.5 μm wavelength band; the average optical depth of water for this range is approximately 40 μm [23], and thus liquid water is opaque for

Table 2
Monolayer equilibrium spreading pressure π_e [8], compressibility C , and Marangoni number Ma computed from Eq. (18).

Surface condition	π_e (mN/m)	C (m/mN)	Ma
Clean [7]	0	∞	0
Oleyl alcohol [28]	29	0.019	1.22
Stearic acid [29]	3	0.0085	1.7
Stearyl alcohol [29]	45	0.0007	52

deeper fluid layers. A calibration was performed prior to experiments to relate the image intensity to temperature to an accuracy of ± 0.082 K according to the procedure developed by Bower et al. [24]. It should be noted that \bar{T}_s is the instantaneous spatial average of all 76,800 pixels in the image (i.e. the average of all $T_s(x,y)$ at time t).

Prior to each experiment, the T_b probe and tank were thoroughly cleaned with reagent grade methanol (>99%, Sigma-Aldrich). The tank was filled to the rim with distilled water, which was heated to approximately 40 °C with an immersion heater. The heater was then removed and the surface was swept free of indigenous surfactant material with a Kimwipe-brand tissue. Use of the IR camera allowed the surface cleanliness to be visually monitored. A pair of IR images of a clean free surface and a surfactant covered surface is shown in Fig. 2a and b, respectively. When the surface was determined to be free of indigenous surfactant material, either a clean surface experiment was initiated, or the surface was prepared with a surfactant monolayer.

Each of the three surfactants required a unique spreading technique. All surfactants used here were insoluble in water. Oleyl alcohol (>99%, Sigma-Aldrich) was applied to the surface in a 50.0 mg/mL solution of heptane (>99% HPLC grade, Sigma-Aldrich) to aid with spreading. Approximately ten times the amount of oleyl alcohol required to reach the equilibrium spreading pressure, π_e , was applied to the surface [25] to account for finite loss of the alcohol from evaporation or dissolution into the water bulk (this quantity is expected to be small). At π_e , the monolayer is in equilibrium with the stable bulk phase, and additional spreading from the bulk will not occur unless the surface pressure π deviates from π_e due to loss of surfactant from the film [7]. Thus, a lens of oleyl alcohol remained at the surface which was available for self-spreading to maintain π_e during the course of an experiment [8]. Similarly, for the stearic acid case a 1.4 mg/mL solution of stearic acid (>98%, Sigma-Aldrich) and heptane was applied to the surface [26]. For stearyl alcohol, the surface was prepared by grinding the solid stearyl alcohol (95%, Acros Organics) into a fine powder [27] and distributing it evenly across the surface at an area concentration of approximately 1.3 g/m². The stearyl alcohol monolayer would spread from these powder flakes, and some solid particles remained undeposited at the interface. In all cases, the surfactant material was allowed to equilibrate on the surface for no less than five minutes before data was acquired. Three experiments were conducted under each of the surfactant conditions for each of the seven tanks. Data was acquired for each surfactant experiment for approximately one hour.

The compressibilities of each of the surfactants used here are presented in Table 2. For oleyl alcohol, Kato et al. [28] determined $C = 0.019$ m/mN, and for stearic acid and stearyl alcohol, respectively, Nutting and Harkins found $C = 0.0085$ m/mN and $C = 0.0007$ m/mN [29]. Hence, stearyl alcohol is the least compressible monolayer used here, and oleyl alcohol is the most compressible. As noted earlier, $C \rightarrow \infty$ for a clean surface.

Computation of h (Eq. (4)) requires the convective heat flux q_c'' leaving through the water surface. For these cool-down experiments, q_c'' is proportional to dT_b/dt (see below). To obtain this derivative, T_b was first fit to an equation, and the derivative obtained

analytically. For the surfactant experiments, T_b was fit to an exponential function of the form:

$$T(t) = (T_i - T_\infty)e^{-t/\tau} + T_\infty \quad (10)$$

where T_i , T_∞ , and τ are fitting parameters representing the initial temperature, a theoretical temperature as $t \rightarrow \infty$, and the temperature decay time constant, respectively. The average standard deviations of T_b from the fit given by Eq. (10) for all runs is $\sigma = 0.02$ °C. The time-rate-change of T_b was computed analytically from the T_b fit from Eq. (10):

$$\frac{dT_b(t)}{dt} = -\frac{1}{\tau}(T_{b,i} - T_{b,\infty})e^{-t/\tau} \quad (11)$$

The procedure and data processing for the clean surface experiments differed from the surfactant experiments. After the warm, distilled water was initially swept free of indigenous surfactant material, the surface would only remain entirely clean for five to ten minutes before contaminating film material would begin to accumulate at the surface again. Whether this surfactant material comes from the water bulk, or the room air remains unclear. On account of this behavior, the duration of each clean surface experiment was dictated by the amount of time that the surface remained surfactant-free, as observed from a second infrared camera which could visualize the entire water surface. Clean surface runs were ended when the formation of a monolayer was observed; often it was the case that small amounts of film would begin to collect in the tank corner, for example. After ending data acquisition, the surfactant material was removed with a tissue and the surface allowed to settle for about one minute after which data acquisition began for the next experiment. At least twelve clean surface experiments were conducted for each tank. Since the rate of change of T_b was relatively constant over these short periods of time, the T_b data were fit to a line as opposed to an exponential function for the longer surfactant runs. The average standard deviation of the T_b data from the linear fit for all clean free surface runs is $\sigma = 0.02$ °C.

The Rayleigh number requires \bar{T}_s in addition to T_b , so the \bar{T}_s data were also fit in the same manner as for T_b . That is, using a linear fit for the clean runs and an exponential fit for the surfactant runs. The average standard deviations of \bar{T}_s from the fits for all runs is $\sigma = 0.05$ °C.

The total heat flux q_t'' was computed using dT_b/dt obtained from derivatives of the fits to T_b according to the equation:

$$q_t'' = -\rho c_p D \frac{dT_b}{dt} \quad (12)$$

where ρ and c_p are the density and specific heat of liquid water, respectively. From q_t'' , the convective heat flux q_c'' was calculated by subtracting the heat loss through the insulated tank walls q_w'' following the procedure of Katsaros et al. [19]. The wall losses for each tank were determined by conducting separate experiments in which an insulated lid was placed on the tank and T_b and T_∞ were

measured as the water cooled. Under this fully-insulated condition, $q_t'' = q_w''$ and the wall losses were known as a function of $T_b - T_\infty$. To determine q_c'' , the wall losses were subtracted from q_t'' according to:

$$q_c'' = q_t'' - \left(\frac{4WD + W^2}{4WD + 2W^2} \right) q_w'' \quad (13)$$

The quantity in parenthesis in Eq. (13) accounts for the losses through the insulated tank bottom and side walls during experiments (and not the free surface). These wall losses account for $\approx 3\%$ of q_t'' . With q_c'' known, Nu data were computed using Eqs. (3) and (4).

Throughout the analysis, T_∞ was regarded as a constant for individual experiments. The temperature dependence of fluid properties was taken into account, and these quantities were evaluated at a temperature equal to the average of T_s and T_b when computing q_c'' , Nu , and Ra . Due to the temperature dependence of ν and α , Pr varied from 3.9 to 5.1 in this investigation. Change in fluid depth D due to evaporation during the course of an experiment was never greater than 0.3 mm, and therefore D was regarded as a constant.

3. Results

Infrared images from the clean surface and surfactant-covered experiments are shown in Fig. 4. The pixel intensities correspond to surface temperature with warmer regions having lighter pixels, and dark pixels indicating relatively cooler regions. The bulk temperature of the water T_b is approximately the same for these four images.

Fig. 5 presents the results from all 63 surfactant runs, and all 103 clean surface runs. Because Nu requires dT_b/dt , which is the analytical derivative of the fit to T_b , Nu is actually a fit. Hence, what is presented in Fig. 5 are fits to Nu and Ra . For the clean surface runs, the fit to T_b is linear. Hence, dT_b/dt is a constant, resulting in a single discrete Nu data point for each run. For the surfactant runs, dT_b/dt is an exponential fit and hence Nu is a fit as well. The fits for these runs are difficult to show in a plot, and thus what is actually presented are the fits with symbols located at intervals.

Note that $NuRa$ is plotted on the ordinate of Fig. 5, as opposed to Nu alone, following the treatment of Globe and Dropkin and others [12,19] enabling removal of the temperature dependence from the y-axis of Fig. 5. This gives:

$$NuRa = q_c'' \frac{g\beta D^4}{\nu\alpha k} \quad (14)$$

With respect to the Nu - Ra relationship, ΔT behaves as the independent parameter during the course of an experiment (and is a quantity in Nu), so it is reasonable to eliminate this from the dependent group Nu . This approach changes the Nu - Ra power law relationship presented in Eq. (8) to:

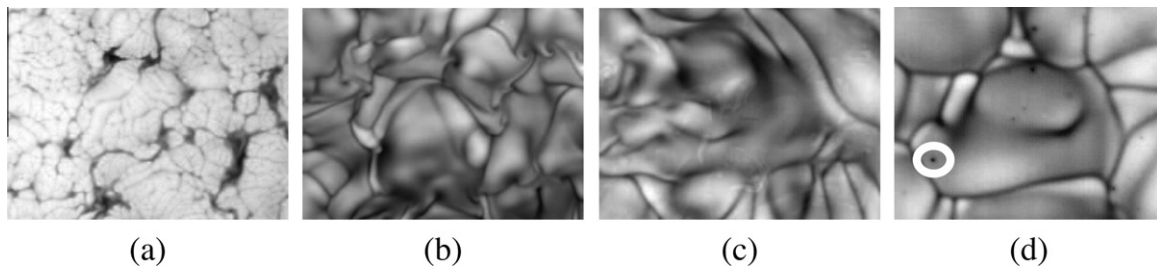


Fig. 4. IR images from experiments with: (a) a clean water surface, (b) an oleyl alcohol covered surface, (c) a stearic acid covered surface, and (d) a stearyl alcohol covered surface with a solid flake of stearyl alcohol indicated by the white circle in the lower-left corner. For all images, the temperature of the underlying water is $T_b \approx 37$ °C. The viewing area is approximately 7.6×5.7 cm.

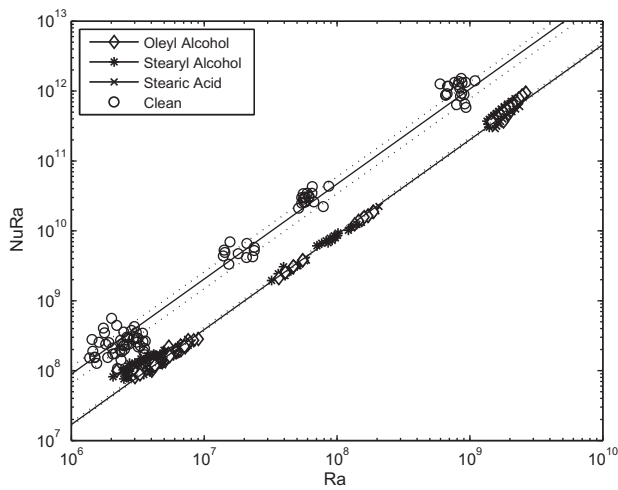


Fig. 5. $Nu-Ra$ results for different surface conditions. The power law fits are given by the solid lines, and the dashed lines indicate the 95% confidence intervals. The upper line is for the clean surface data (open circles). The power law and confidence interval lines are indistinguishable for the different surfactant data, and thus only stearic acid is shown.

Table 3

A summary of the $Nu-Ra$ power law scalings A and m determined from a regression analysis of the experimental data. The 95% confidence intervals for the fits are provided. A^* was determined for each by forcing the exponent to the average $\bar{m} = 0.363$ and re-fitting the data. The heat transfer coefficient ratio is computed from Eq. (17).

Surface condition	A	m	$CI_{95\%}$ (%)	A^*	\mathcal{H}
Clean	0.492	0.362	28.7	0.487	0
Oleyl alcohol	0.071	0.376	7.5	0.092	-.81
Stearic acid	0.090	0.361	7.8	0.087	-.82
Stearyl alcohol	0.110	0.356	9.4	0.096	-.80

$$NuRa = A \cdot Pr^{0.074} Ra^{(m+1)} \quad (15)$$

The power law exponent increases from m in Eq. (7) to $m + 1$ in Eq. (15).

The results presented in Fig. 5 show that Nu is significantly larger for the clean surface case than for any of the surfactant cases; this is true over the entire four decades in Ra explored here. This difference in Nu is approximately one order of magnitude, showing that surfactants (at least those explored here) significantly reduce the efficiency of heat transfer on the water-side of an air/water interface during natural convection. The difference between the three surfactant conditions was surprisingly small. Indeed, in Fig. 5, the difference between the fits for each of the three surfactant cases is so small that they appear as a single solid line. Why this should be the case is addressed in the following section. The relatively large scatter in the clean surface data is likely due to the linear fitting of T_b data being affected by low frequency fluctuations of T_b caused by the motion of warm and cool plumes passing over the T_b probe during these short duration runs.

The power law fits presented in Fig. 5 and Table 3 were obtained via linear fits to the logarithms of $Nu \cdot Ra$ and Ra (i.e. the logarithm of both sides of Eq. (15)):

$$\log(Nu \cdot Ra) = \log(A) + 0.074\log(Pr) + (m + 1)\log(Ra) \quad (16)$$

The number of experiments conducted at the shallowest depth D (i.e. the lowest range of Ra) was approximately four times greater than the number of experiments for any other D ; this was due to the fact that four different tanks widths W were explored for $D = 5$ cm. For this reason, the data were weighted during the linear

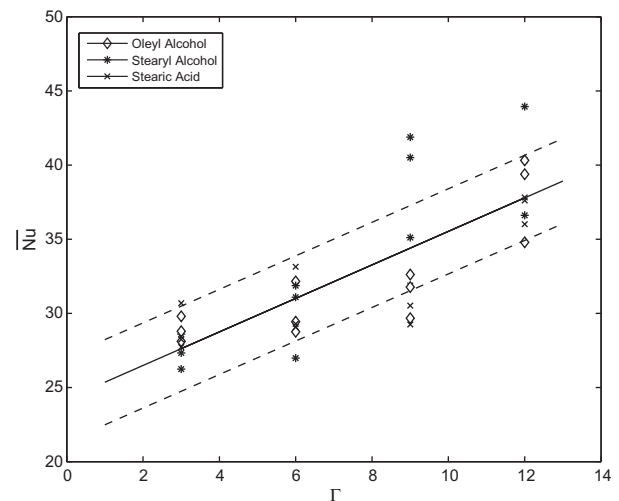


Fig. 6. Average Nu vs. aspect ratio Γ for the surfactant runs of $D = 5$ cm at $Ra \approx 5 \times 10^6$. A linear fit to the data is provided to show the increasing trend of \bar{Nu} with Γ , and the dashed lines indicate the standard deviation of the data from the fit.

regression analysis so that Nu data for all four ranges of Ra were evenly represented.

The distance between the dotted lines in Fig. 5 is equal to the 95% confidence interval, reflecting the deviation of the data from the $Nu-Ra$ power law fits and the measurement uncertainties and fitting error associated with T_b and \bar{T}_s . Table 3 summarizes these confidence intervals. The clean surface case has the largest Nu confidence interval on account of the relatively large scatter in the data, and also the difficulty in \bar{T}_s measurement as $\Delta T \rightarrow 0$; the bulk water temperature T_b was measurable within ± 0.01 °C compared to \bar{T}_s which is only known to within ± 0.082 °C. The average value of ΔT for all clean experiments is $\bar{\Delta T} = 0.48$ °C, compared to $\bar{\Delta T} \approx 1.0$ °C for the surfactant runs. The uncertainty in \bar{T}_s can therefore affect ΔT by as much as almost 20% for the clean cases, and by no more than 10% for the surfactant conditions.

As shown in Table 1, for the shallowest tank ($D = 5$ cm) four different tank widths were investigated. This gives four different aspect ratios, Γ (Eq. (9)) for the same tank depth D . This is useful since, while ΔT obviously changes the value of Ra , it is D in this work which has the biggest effect on the magnitude of Ra . Hence, the average of Nu can be computed for each of the $D = 5$ cm tanks and plotted against Γ to reveal the effect of aspect ratio on \bar{Nu} for nominally fixed Ra . This is presented in Fig. 6, where each $D = 5$ cm tank run is represented by a single marker because \bar{Nu} is presented, which is the average Nu for the duration of the experiment. The trend line gives $Nu(\Gamma = 3) \approx 28$ and $Nu(\Gamma = 12) \approx 39$, which is roughly a 40% increase in Nu . The significance of this result is presented in the following section.

4. Discussion

The main findings of this experimental investigation are: (1) Nu is nearly an order of magnitude greater for the clean surface case than for any of the surfactant conditions, (2) Nu for the three surfactant cases are about the same in spite of differences in compressibility C , and (3) for all surface conditions explored here, the power laws show that $m > 1/3$ for all cases, which is uniquely different from the results of many Rayleigh-Bénard studies. Additionally, these experiments show that, for nominally constant Ra , Nu increases with aspect ratio Γ . These findings are now further discussed.

First, the presence of the surfactant monolayers reduced Nu by approximately a factor of ten from the clean surface condition case

as observed in Fig. 5. That is, when any of the surfactant monolayers were present at the air/water interface, the efficiency of convective exchange was reduced. The effect of the surfactants on Nu is quantified, in part, by the differences in the Nu – Ra coefficient A from that of the clean case in Table 3. The clean surface condition gives $A = 0.492$ while all surfactant cases yield A that are smaller by more than a factor of four. This indicates that, over the range of Ra explored here, convective heat transfer occurs more efficiently in the absence of a surfactant monolayer; this is likely due to the convective motion being physically impeded by a shear-yielding hydrodynamic boundary at the interface when a surfactant is present. To quantify the reduction in the heat transfer coefficient h relative to the clean surface case h_o on account of the surfactant monolayers, we define a heat transfer coefficient ratio \mathcal{H} :

$$\mathcal{H} = \left(\frac{h - h_o}{h_o} \right)_{Ra, D, \bar{m}} = \frac{A^* - A_o^*}{A_o^*} \quad (17)$$

The quantity shown in Eq. (17) can be derived by expanding and rearranging the terms in Eq. (8). We have evaluated the heat transfer coefficients in Eq. (17) at equivalent Ra , D , and \bar{m} . The coefficient A^* was determined by re-fitting the data for each case with the Nu – Ra exponent forced to $\bar{m} = 0.363$, the average m for all cases. If the actual m shown in Table 3 were used to compute \mathcal{H} , then \mathcal{H} would vary with Ra since no two m are equal. Thus, \mathcal{H} shown in Table 3 is a simplified approximation of the decrease in the heat transfer coefficient on account of the surfactant monolayers. When these surfactants are added to a clean free surface, the heat transfer coefficient is reduced by 80%. This is clear evidence that surfactant monolayers increase the fluid body's resistance to heat transfer.

The ability of the surfactant monolayers to reduce the efficiency of heat transfer can be observed in the IR images in Fig. 4. The structures seen in the images are indicative of the natural convection motion beneath the surface; warm plumes of water rise to the interface and, upon cooling, the water collects into slender sheet-like regions and plunges back down into the bulk. Fine, turbulent structures are present in Fig. 4(a) when the surface is clean, and the convective motion occurs at a relatively quick pace. A dramatic change of the spatial scales is exhibited in Fig. 4(b), (c), and (d) when surfactant monolayers of oleyl alcohol, stearic acid, and stearyl alcohol, respectively, cover the surface. The absence of the small turbulent structures in the surfactant images indicates that the surfactants are decreasing surface mobility and are damping out some of the turbulence exhibited under the clean surface condition. That is, the convective motion at the surface is observed to decrease when a surfactant covers the interface. This observation relates to Fig. 5 in that convective transport of heat proceeds unimpeded for the clean surface case which yields Nu that are greater than Nu of any of the surfactant covered surface conditions by nearly a factor of ten.

Secondly, although there is a significant difference between the Nu – Ra behavior of the clean surface and surfactant covered surface conditions, there is no measurable difference in the Nu – Ra data among the three surfactant cases even though the compressibility C vary by up to a factor of 27 (see Table 2). Within the confidence limits of the data, the behavior of natural convection can be described with essentially the same Nu – Ra power law for the conditions of oleyl alcohol, stearic acid, and stearyl alcohol covered surfaces. The average Nu – Ra power law of the surfactant data in Table 3 is $Nu = 0.090Ra^{0.364}$. This overlapping behavior of the three surfactant conditions indicates that the monolayers all have an approximately equal effect on convection beneath a free surface.

This result was initially surprising to the authors due to the variation of C and the seemingly different behaviors that were observed between the surfactants in the IR imagery. The stearic acid and stearyl alcohol monolayers have a unique rigid quality

due to their low compressibility C which cannot be observed in still images. Small surface defects can be visualized in IR video of stearic acid and stearyl alcohol (the solid flake of stearyl alcohol in the lower left quadrant of Fig. 4(d), for example) which remain relatively “locked” in place at the interface throughout the duration of a run although the fluid underneath is in convective motion. Over the course of one hour, the location of the surface defects might appear to change by only 1 cm. This behavior is evidence that stearic acid and stearyl alcohol monolayers impose what is essentially a no-slip boundary condition at the air/water interface. The oleyl alcohol surfactant monolayer does not exhibit this rigid behavior, and appears to deform (albeit slowly) in a compressible manner as also observed in the IR by Flack et al. [2]. It is possible that for each of the surfactant cases the time scale at which surface deformation occurs is large relative to the time scale of the convective motion beneath the surface. That is, even though surface deformation is observed with oleyl alcohol, it is occurring at a slower rate than the underlying fluid motion, and in this manner oleyl alcohol imparts a boundary condition that is comparable to the rigid, no-slip behavior of stearic acid and stearyl alcohol. Visual comparison of IR video of the rapid, turbulent nature of a clean surface condition with the sluggish nature of the surfactant conditions supports this idea, and would explain why all three surfactants inhibit convection to approximately the same degree.

That all three surfactants yield a similar effect on Nu relative to the clean case is supported by the computational results of Shen et al. [30] who found that deviation from a clean surface condition on account of even slight contamination by surfactants will reduce near-surface turbulent transport. Shen et al. [30] explored the surfactant boundary condition with the Marangoni number, Ma :

$$Ma = \frac{a}{\sigma} \frac{\partial \sigma}{\partial a} = \frac{1}{\sigma C} \quad (18)$$

where σ is the surface tension and C is the compressibility defined in Eq. (1). Table 2 gives Ma for the surface conditions investigated here. Shen et al. [30] found that as Ma increased due to increasing quantities of surfactant material at the surface, the velocity fluctuation near the air/water interface decreased gradually; there was observed to be a sharp decrease, however, in the surface divergence as Ma increased to around $Ma \propto 10^{-3}$; in fact, the reduction in upwelling and downwelling approaches a maximum and becomes essentially independent of Ma above $Ma \propto 10^{-3}$. Table 2 shows that all surfactant monolayers from the current work give Ma that are orders of magnitude greater than the critical value $Ma \propto 10^{-3}$ observed by Shen et al. [30]. This can explain why the surfactants have shown a significant and seemingly equal effect on Nu – Ra here although C are different.

Thirdly, the Nu – Ra exponents m given in Table 3 were greater for all four surface conditions than $m \approx 1/3$ which is commonly reported in Nu – Ra studies. The Nu – Ra results from previous studies are shown in Table 4 for comparison. The larger exponent m found in this study indicates that the rate at which Nu increases with Ra is greater under a free surface condition compared to Rayleigh–Bénard convection between solid walls. The authors acknowledge that the nature of turbulent transport in our experiments is highly three-dimensional, but it is worth mentioning that Moore and Weiss [31] found $Nu \propto Ra^{0.365}$ in their numerical study of convection between two free boundaries. This suggests, perhaps, that $m > 1/3$ is characteristic of natural convection with free boundaries.

The Nu – Ra results from this study are compared with earlier studies in Fig. 7 and Table 4. For all studies of the Rayleigh–Bénard type, the authors have adjusted the published coefficients A following the treatment of Katsaros et al. [19] and Prasad [32]. This adjustment transforms the Rayleigh–Bénard rigid boundary coefficient A_{RB} to a coefficient comparable to a free surface coefficient A^\dagger :

Table 4
A summary of the Nu – Ra power law scalings A and m from different studies of convection beneath an air/water interface. For the current results, $A = A \cdot \overline{Pr}^{0.074}$ where $\overline{Pr} = 4.3$ is the average from experiments. The coefficient A in the study of Navon and Fenn [13] has been estimated based on the data presented in their figure. The Rayleigh–Bénard (R–B) coefficients have been transformed according to Katsaros et al. [19] with Eq. (19) for free surface comparison, and are denoted with the superscript †.

$Nu = ARa^m$				
Study	Condition	A	m	Ra range
Current	Clean	0.548	0.362	$1 \times 10^6 < Ra < 1 \times 10^9$
	Oleyl	0.079	0.376	$2 \times 10^6 < Ra < 3 \times 10^9$
	Stearic	0.100	0.361	$2 \times 10^6 < Ra < 3 \times 10^9$
	Stearyl	0.122	0.356	$2 \times 10^6 < Ra < 3 \times 10^9$
	Clean	0.052	1/3	$1.5 \times 10^4 < Ra < 2.5 \times 10^5$
Navon and Fenn [13]	Clean	0.052	1/3	$4 \times 10^8 < Ra < 4 \times 10^9$
Katsaros et al. [19]	Clean	0.156	1/3	$2.2 \times 10^4 < Ra < 1.1 \times 10^7$
Federico and Foraboschi [14]	Free	0.092	1/3	$1.51 \times 10^5 < Ra < 6.76 \times 10^8$
Globe and Dropkin [12]	R–B	0.077	1/3	$1.51 \times 10^5 < Ra < 6.76 \times 10^8$
Chu and Goldstein [33]	Free†	0.186	1/3	$2.76 \times 10^5 < Ra < 1.05 \times 10^8$
	R–B	0.183	0.278	$2.76 \times 10^5 < Ra < 1.05 \times 10^8$
	Free†	0.444	0.278	$2.76 \times 10^5 < Ra < 1.05 \times 10^8$
Malkus [34]	R–B	0.083	0.325	$5 \times 10^5 < Ra < 1 \times 10^8$
	Free†	0.208	0.325	$5 \times 10^5 < Ra < 1 \times 10^8$
Niemela et al. [35]	R–B	0.124	0.309	$1 \times 10^6 < Ra < 1 \times 10^{17}$
	Free†	0.307	0.309	$1 \times 10^6 < Ra < 1 \times 10^{17}$

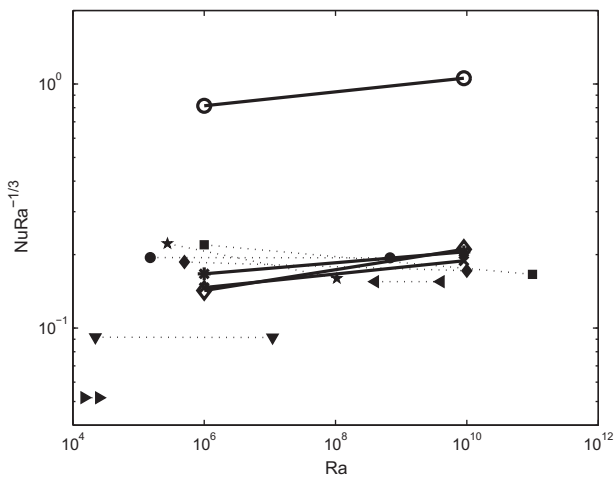


Fig. 7. A comparison of Nu – Ra results. The results of the current study are given by the bold solid lines and the same symbols as in Fig. 5 to indicate surface condition. The earlier studies are given by the dotted lines and are distinguished by the solid-faced symbols: (►) Navon and Fenn [13], (▼) Federico and Foraboschi [14], (◄) Katsaros et al. [19], (■) Niemela et al. [35], (◆) Malkus [34], (★) Chu and Goldstein [33], and (●) Globe and Dropkin [12].

$$A^\dagger = A_{RB}2^{(1+m)} \quad (19)$$

Katsaros et al. [19] apply this treatment by assuming that, across depth D , the ΔT for a free surface study is exactly half of the ΔT in a Rayleigh–Bénard study at equivalent heat flux q_c' . A schematic of this free surface/Rayleigh–Bénard comparison is given in Fig. 1. This treatment in Eq. (19) was only applied to the Nu – Ra results of earlier Rayleigh–Bénard studies; the results of free surface studies were not adjusted.

It should be noted that Navon and Fenn [13] did not present their coefficient A and only indicated that $Nu \approx Ra^{1/3}$. We have estimated their value of A by performing a linear regression of several Nu and Ra data that, to the best of our ability, we measured from the Nu – Ra figure presented in their paper; we approximate that the data due to Navon and Fenn is represented by $Nu = 0.052Ra^{1/3}$ for a clean free surface.

In Fig. 7 the y -axis Nu has been normalized by $Ra^{1/3}$. It can be shown from Eq. (8) that this treatment equates to:

$$\frac{Nu}{Ra^{1/3}} = A \cdot Pr^{0.074} Ra^{(m-1/3)} \quad (20)$$

Thus if $m = 1/3$, then $Nu \cdot Ra^{-1/3} = A \cdot Pr^{0.074}$ exactly for all Ra and the data will appear as a horizontal line in Fig. 7. Presenting the data in this form clearly indicates deviation from $m = 1/3$ and also distinguishes the differences in the coefficient A . Since most of the exponents presented are close to $1/3$, the main difference between the various studies is A (and A^\dagger), or the location of the data on the y -axis of Fig. 7.

In Fig. 7 there is a large disparity between the current clean surface data, and the clean surface data from the free surface studies of Katsaros et al. [19] and Navon and Fenn [13]. As discussed earlier, the authors question whether or not a clean free surface was fully achieved and maintained during these two prior investigations. It is clear from current results that the presence of a monolayer will add significant resistance to the convective motion of a fluid. Because the Nu – Ra result from Katsaros et al. [19] is very close to all of our surfactant results, we believe that the clean surface experiments of Katsaros et al. were indeed affected by indigenously surfactant material that formed at the surface after the initial surface cleaning procedure. Thus, it is reasonable to believe that the Nu – Ra result of Katsaros et al. [19] is representative of convection beneath a surfactant-laden free surface.

Discussion is owed to the difference between the thermal conditions at the upper boundary in the current study and the Rayleigh–Bénard studies due to Chu and Goldstein [33], Globe and Dropkin [12], Malkus [34] and Niemela et al. [35]. In a Rayleigh–Bénard study, the upper and lower boundaries are typically thick, temperature regulated plates with good thermal conductivity and a large thermal capacity. As plumes of warm and cool fluid contact these boundaries, the plates develop local warm and cool regions which tend to be homogenized by the lateral exchange of heat within the plates. In this manner, the plates deviate only slightly from the ideal isothermal condition during experiments. Constant heat flux boundary conditions can be obtained by bonding a constant resistance heater to the surface of an insulating material. Several researchers have investigated the problem of convection between plates of constant temperature and constant heat flux boundary conditions [36,37]. Chillà et al. [37] discuss that unstable plate temperatures can interfere with heat transport in the fluid. Verzicco and Sreenivasan [36] examine the flow dynamics of isothermal and constant heat flux boundary conditions, and note that temperature fluctuations in the heated lower plate can cause rising plumes to be cooler and consequently transport less heat than the isothermal case. Verzicco and Sreenivasan [36] argue that typical Rayleigh–Bénard experimental conditions for the lower heated

plate are closer to the constant heat flux case than the isothermal boundary condition.

In these free surface experiments, heat traverses the bulk via convection and is dumped at the air/water interface where the surface cools primarily from evaporation and convective transfer to the cooler ambient surroundings; the water vapor and sensible heat is quickly advected away from the surface and is dissipated in the ambient. In contrast to a Rayleigh–Bénard experiment, there is very little tendency for the temperature to homogenize at the free surface since there is no highly conductive solid plate to diffuse energy laterally and flatten temperature gradients. The authors posit that the thermal condition at the free surface is responsible for the larger exponent m compared to the Rayleigh–Bénard studies which tend more towards having isothermal boundaries. It may be the case that surface temperature inhomogeneity at the air/water interface is permitting the formation of small, localized plumes of air above the warm surface regions which entrain heat from surrounding areas. This air-side behavior due to surface temperature gradients may be increasing the overall efficiency of global water-side convective transport.

Lastly, a dependence of Nu on the aspect ratio Γ was observed for the $D = 5$ cm tanks. The data obtained from these tanks corresponds to the clump of data at the lowest Ra in Fig. 5 ($Ra \approx 5 \times 10^6$). The effect of Γ on Nu is shown in Fig. 6 for the surfactant runs on all tanks of $D = 5$ cm. It is evident from Fig. 6 that, although the runs are at approximately the same Ra , there is a slight monotonically increasing trend of Nu with Γ . In designing the experiments, the authors initially believed that Nu would be independent of Γ , and thus a variety of Γ would be acceptable due to the work of Deardorff and Willis [38]. Deardorff and Willis [38] conducted convection experiments in a Rayleigh–Bénard type setup and showed for several Ra and a range of $0.1 < \Gamma < 20$ that Nu was unaffected by Γ so long as $\Gamma > 2$. In this free surface study, however, Fig. 6 shows that Nu is not independent of Γ even for Γ as large as twelve. If one considers that the convective motion of the air above the free surface is similar to the convective flow above a heated flat plate, then it is true that as the horizontal extent W increases (and thus Γ increases for a given D as shown in Fig. 6), air-side convective heat transfer increases as well. This increase in air-side q_c'' may also be increasing the water-side Nu which could explain the trend seen in Fig. 6.

5. Conclusion

In this study, we have investigated the effects of several surfactant monolayers on the convective behavior of a heated water body with a free upper surface. Importantly, an IR camera was used to visualize the different surface conditions and to verify the existence of a clean free surface.

Three decades of Ra were explored in a set of tanks by varying D for different surface conditions. The Nu – Ra power law relationships were computed from the data, and all surface conditions yield an exponent $m > 1/3$. The coefficient A for the oleyl alcohol, stearic acid, and stearyl alcohol surface conditions were all close to approximately $A = 0.090$, and the clean surface condition coefficient gave a larger coefficient of $A = 0.492$. The difference in A indicates that natural convection heat transfer is more efficient when the air/water interface is free of surfactants, i.e. clean. The addition of a surfactant monolayer to a clean free surface will inhibit the convective motion in the subsurface region as the boundary condition tends toward the no-slip type and water near the interface is immobilized. This effect at the free surface boundary reduces the heat transfer coefficient h by as much as 80% compared to the case of a clean surface condition.

The Nu – Ra exponent m for all surface conditions was larger than $m \approx 1/3$ typically found in Rayleigh–Bénard studies. The

authors believe that this may be attributed to the difference in the thermal boundary conditions. For the Rayleigh–Bénard case, surface temperature gradients at the boundaries are quickly eliminated via lateral conduction within the solid plates and the plate temperatures tend towards homogeneity. For the case of the free surface studied herein, heat is quickly advected away from the air/water interface and the surface temperature field maintains inhomogeneity. Enhanced air-side convection due to local warm regions may be causing the water-side convection to increase at a greater rate with Ra .

A dependence of Nu upon aspect ratio Γ was also discovered at the lowest range of $Ra \approx 5 \times 10^6$. This finding contrasts the earlier work of Deardorff and Willis [38] who found Nu and Γ to be independent.

Acknowledgments

This research was supported by the National Science Foundation, and the Department of Energy through the Savannah River National Laboratory. Support from these agencies is gratefully acknowledged.

References

- [1] J.R. Saylor, G.B. Smith, K.A. Flack, Infrared imaging of the surface temperature field of water during film spreading, *Phys. Fluids* 12 (2000) 597–602.
- [2] K.A. Flack, J.R. Saylor, G.B. Smith, Near surface turbulence for evaporative convection at an air/water interface, *Phys. Fluids* 13 (2001) 3338–3345.
- [3] G.E. Lau, G.H. Yeoh, V. Timchenk, J.A. Reizes, Large-eddy simulation of turbulent natural convection in vertical parallel-plate channels, *Numer. Heat Transfer, Part B: Fundam.* 59 (2011) 259–287.
- [4] R.J. Goldstein, W.E. Ibele, S.V. Patankar, T.W. Simon, T.H. Kuehn, P.J. Strykowski, K.K. Tamma, J.V.R. Heberlein, J. Bischof, F.A. Kulacki, U. Kortshagen, S. Garrick, V. Srinivasan, K. Ghosh, R. Mittal, Heat transfer – A review of 2005 literature, *Int. J. Heat Mass Transfer* 53 (2010) 4397–4447.
- [5] W.D. Harkins, *The Physical Chemistry of Surface Films*, Reinhold Publishing Corporation, New York, 1952.
- [6] J.T. Davies, E.K. Rideal, *Interfacial Phenomena*, second ed., Academic Press, 1963.
- [7] G.L. Gaines Jr., *Insoluble Monolayers at Liquid–Gas Interfaces*, John Wiley & Sons, New York, NY, 1966.
- [8] V.K. La Mer (Ed.), *Retardation of Evaporation by Monolayers: Transport Processes*, Academic Press, New York, 1962.
- [9] N.L. Jarvis, The effect of monomolecular films on surface temperature and convective motion at the water/air interface, *J. Colloid Sci.* 17 (1962) 512–522.
- [10] N.L. Jarvis, R.E. Kagarise, Determination of the surface temperature of water during evaporation studies. A comparison of thermistor with infrared radiometer measurements, *J. Colloid Sci.* 17 (1962) 501–511.
- [11] K.B. Katsaros, W.D. Garrett, Effects of organic surface films on evaporation and thermal structure of water in free and forced convection, *Int. J. Heat Mass Transfer* 25 (1982) 1661–1670.
- [12] S. Globe, D. Dropkin, Natural-convection heat transfer in liquids confined by two horizontal plates and heated from below, *J. Heat Transfer* 81 (1959) 24–28.
- [13] U. Navon, J.B. Fenn, Interfacial mass and heat transfer during evaporation: I. An experimental technique and some results with a clean water surface, *AIChE J.* 17 (1971) 131–136.
- [14] I. Federico, F.P. Foraboschi, A contribution to the study of free convection in a fluid layer heated from below, *Int. J. Heat Mass Transfer* 9 (1966) 1351–1360.
- [15] U. Navon, J.B. Fenn, Interfacial mass and heat transfer during evaporation: II. Effect of monomolecular films on natural convection in water, *AIChE J.* 17 (1971) 137–140.
- [16] G.T. Barnes, Optimum conditions for evaporation control by monolayers, *J. Hydrol.* 145 (1993) 165–173.
- [17] G.T. Barnes, Role of monolayers in evaporation retardation, *Nature* 220 (1968) 1025–1026.
- [18] F. Sebba, H.V.A. Briscoe, The evaporation of water through unimolecular films, *J. Chem. Soc.* 1 (1940) 106–114.
- [19] K.B. Katsaros, W.T. Liu, J.A. Businger, J.E. Tillman, Heat transport and thermal structure in the interfacial boundary layer measured in an open tank of water in turbulent free convection, *J. Fluid Mech.* 83 (1977) 311–335.
- [20] J.R. Saylor, Determining liquid substrate cleanliness using infrared imaging, *Rev. Sci. Instrum.* 72 (2001) 4408–4414.
- [21] J.R. Saylor, G.B. Smith, K.A. Flack, An experimental investigation of the surface temperature field during evaporative convection, *Phys. Fluids* 13 (2001) 428–439.
- [22] J.R. Saylor, G.B. Smith, K.A. Flack, The effect of a surfactant monolayer on the temperature field of a water surface undergoing evaporation, *Int. J. Heat Mass Transfer* 43 (2000) 3073–3086.

- [23] M.R. Querry, D.M. Wieliczka, D.J. Segelstein, Water (H₂O), in: E.D. Palik (Ed.), *Handbook of Optical Constants of Solids II*, Academic Press, San Diego, 1998, pp. 1059–1077.
- [24] S.M. Bower, J.R. Saylor, A study of the Sherwood–Rayleigh relation for water undergoing natural convection-driven evaporation, *Int. J. Heat Mass Transfer* 52 (2009) 3055–3063.
- [25] M.J. Vogel, A.H. Hirs, Concentration measurements downstream of an insoluble monolayer front, *J. Fluid Mech.* 472 (2002) 283–305.
- [26] W.D. Harkins, J.W. Morgan, Polymolecular and monomolecular films, *Proc. National Acad. Sci. U.S.A.* 11 (1925) 637–643.
- [27] F. MacRitchie, Evaporation retardation by monolayers, *Science* 163 (1969) 929–931.
- [28] T. Kato, K. Seki, R. Kaneko, Insoluble monolayers of irisquinone and its related substances at the air/water interface, *J. Colloid Interface Sci.* 109 (1986) 77–89.
- [29] G.C. Nutting, W.D. Harkins, Pressure-area relations of fatty acid and alcohol monolayers, *J. Am. Chem. Soc.* 61 (1939) 1180–1187.
- [30] L. Shen, K.P. Yue, G.S. Triantafyllou, Effect of surfactants on free-surface turbulent flow, *J. Fluid Mech.* 506 (2004) 79–115.
- [31] D.R. Moore, N.O. Weiss, Two-dimensional Rayleigh–Bénard convection, *J. Fluid Mech.* 58 (1973) 289–312.
- [32] A.K. Prasad, Derivation of Rayleigh number for nonpenetrative thermal convection, *J. Heat Transfer* 119 (1997) 180–183.
- [33] T.Y. Chu, R.J. Goldstein, Turbulent convection in a horizontal layer of water, *J. Fluid Mech.* 60 (1973) 141–159.
- [34] W.V.R. Malkus, Discrete transitions in turbulent convection, *Proc. Roy. Soc. A* 225 (1954) 185–195.
- [35] J. Niemela, L. Skrbek, K. Sreenivasan, R. Donnelly, Turbulent convection at very high Rayleigh numbers, *Nature* 404 (2000) 837–840.
- [36] R. Verzicco, K.R. Sreenivasan, A comparison of turbulent thermal convection between conditions of constant temperature and constant heat flux, *J. Fluid Mech.* 595 (2008) 203–219.
- [37] F. Chillà, M. Rastello, S. Chaumat, B. Castaing, Ultimate regime in Rayleigh–Bénard convection: the role of plates, *Phys. Fluids* 16 (2004) 2452–2456.
- [38] J.W. Deardorff, G.E. Willis, The effect of two-dimensionality on the suppression of thermal turbulence, *J. Fluid Mech.* 23 (1965) 337–353.
- [39] R.J. Adrian, R.T.D.S. Ferreira, T. Boberg, Turbulent thermal convection in wide horizontal fluid layers, *Exp. Fluids* 4 (1986) 121–141.